Ethene Polymerization Activity and Coordination Gap Aperture in non-*ansa* Alkyl-Substituted Cyclopentadienyl- and Phospholyl-Zirconium/MAO Catalysts☆

Christoph Janiak*[a], Katharina C. H. Lange[a], Uwe Versteeg[a], Dieter Lentz[b], and Peter H. M. Budzelaar[c]

Institut für Anorganische Chemie, Technische Universität Berlin[a],
Straße des 17. Juni 135, D-10623 Berlin, Germany
Telefax: (internat.) +49(0)30314-22168

Institut für Anorganische und Analytische Chemie, Freie Universität Berlin[b],
Fabeckstraße 34–36, D-14195 Berlin, Germany

Department of Inorganic Chemistry, University of Nijmegen[c],
P. O. Box 9010, 6500 GL Nijmegen, The Netherlands

Received June 28, 1996

Key Words: Zirconocenes / Metallocene-methylalumoxane catalysts / Ethene polymerization / Structure–reactivity correlation / Coordination gap aperture / Cone angles / ^{91}Zr NMR

The ethene polymerization activities of a series of $Cp'(C_5H_5)ZrCl_2$ and Cp'_2ZrCl_2 pre-catalysts ($Cp' = C_5HMe_4$, C_4Me_4P, C_5Me_5, C_5H_4tBu, C_5H_3-1,3-tBu_2, C_5H_2-1,2,4-tBu_3) together with $(C_5H_5)_2ZrCl_2$ have been correlated with the coordination gap aperture. In the case of the mixed substituted $C_5R_{5-n}R'_n$ ligands, the coordination gap aperture has been determined with the help of the cyclopentadienyl cone angle and the bending angle at zirconium. A hindered rotatability of the *tert*-butyl substituted systems has been evaluated by molecular modeling calculations and was included in the gap aperture estimation. Deviations from the activity–gap aperture correlation in the case of the phospholyl (C_4Me_4P) systems could be accounted for in terms of adduct formation between aluminum species and the phosphorus donors. These Lewis acid/base adducts form in an equilibrium reaction at high Al/Zr ratios, as shown by ^{31}P NMR. Ab initio calculations on model L_2TiMe^+ complexes ($L = C_5H_5$, C_5H_4N and C_5H_4P) for the insertion of ethene in the Ti–Me bond suggest a high electronic similarity for phospholyl and cyclopentadienyl. The ^{91}Zr-NMR data (chemical shift and line width) for the above zirconocene series are reported. The ^{91}Zr chemical shift values increase with a good linear correlation to the number of methyl or *tert*-butyl groups, which is traced to the additive electron donating effect of the alkyl groups. The hyperconjugative donor effect of a *tert*-butyl group is found here to be 1.25 times that of a methyl group. The X-ray structure of $(C_5H_3$-1,3-$tBu_2)(C_5H_5)ZrCl_2$ has been determined (monoclinic, $P2_1/n$, $a = 6.631(3)$, $b = 18.843(9)$, $c = 15.265(5)$ Å, $\beta = 91.3°$, $Z = 4$).

Introduction

Single-site metallocene-methylalumoxane (MAO) catalysts are currently being introduced in industry as a new generation of Ziegler-Natta catalysts for the polymerization of olefins[1–3]. Relationships between the structures of the zirconocene complexes and their properties as polymerization catalysts are of central interest in the majority of studies in this area[3–9]. Determinations of the steric (and electronic) parameters of zirconocenes and their correlations with activity have been reported[10–13]. The most successful approach to such a correlation appears to be the use of the coordination gap aperture (Figure 1) put forward by Brintzinger et al.[13]. We have used this concept in a systematic study concerning the comparative performance of methyl- and *tert*-butyl-substituted zirconocenes in ethene polymerization. Metal complexes bearing bulky cyclopentadienyl ligands often exhibit properties different from those of the corresponding unsubstituted cyclopentadienyl analogs[14]. Here we report the coordination gap apertures, ^{91}Zr-NMR chemical shifts, and the ethene polymerization activity (in combination with MAO) of 11 different systematically alkyl-substituted zirconocenes (**2**–**12**). The unsubstituted parent system zirconocene dichloride (**1**) was included as a reference point.

Results

Coordination Gap Apertures

This geometric parameter is defined as "the largest possible angle spanned by those two planes through the metal center which touch the inner van der Waals outline of each of the C_5-ring ligands" (cf. Figure 1)[13]. At the beginning of our study, our aim was a determination of the coordination gap apertures for the zirconocenes **1**–**12**. Only the gap apertures for compounds **1**, **6** and **7**, which contain the fivefold symmetrical C_5H_5 or C_5Me_5 ligands, could be obtained by simply drawing the van der Waals outlines based on the experimental X-ray structural geometries and measuring the opening angle. The gap apertures for complexes with the unsymmetrical substituted C_5HMe_4, C_4Me_4P, and the various *tert*-butylcyclopentadienyl ligands were not accessible in this way due to the different rotamers possible. To average the gap aperture for the different ring rotamers we utilized the cyclopentadienyl ring cone angles with the metal as apex of the cone (Figure 2). This cyclopentadienyl

  0009–2940/96/1212–1517 $ 15.00+.25/0

Scheme 1. Methyl-substituted zirconocene dichlorides and parent zirconocene dichloride used in the catalytic studies

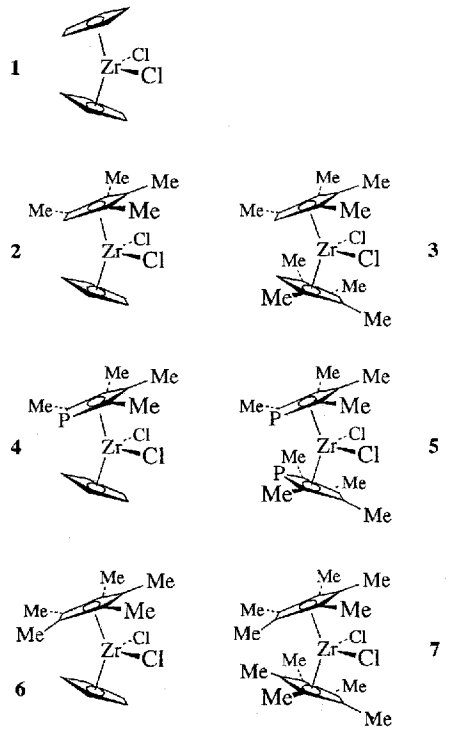

Scheme 2. *tert*-Butyl-substituted zirconocene dichlorides used in the catalytic investigations

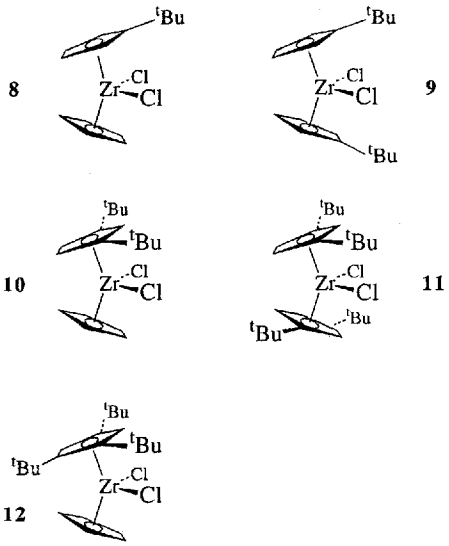

cone angle concept has been used for steric measurement of substituted cyclopentadienyl ligands and has also been employed to explain differences in ethene polymerization activities among $(C_5H_4R)_2TiCl_2$ and $(C_5H_4R)(C_5H_5)TiCl_2$/$Et_3Al_2Cl_3$ and among $(C_5H_4R)_2ZrCl_2$/ethylalumoxane catalysts[5,10–12,15]. When the cone angle α is known for a substituted cyclopentadienyl ligand, the coordination gap aperture (cga) can then be calculated with the help of the bending angle β at zirconium, according to equation 1 (cf. Figure 3). The bending angle is taken here as the ring-centroid–metal–ring-centroid angle.

Figure 1. Schematic representation of the coordination gap aperture (cga) of a bent metallocene based on the van der Waals surface of the ring ligands. The gap aperture means the maximum opening angle; for clarity only the van der Waals surfaces of the ring substituents (circles) along the maximum opening are shown

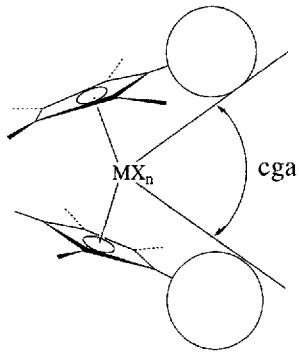

Figure 2. Schematic illustration of the cone angle α of a metal-bound cyclopentadienyl ligand. The circles represent the van der Waals outlines of the ring substituents; note that α depends on the metal–ring distance

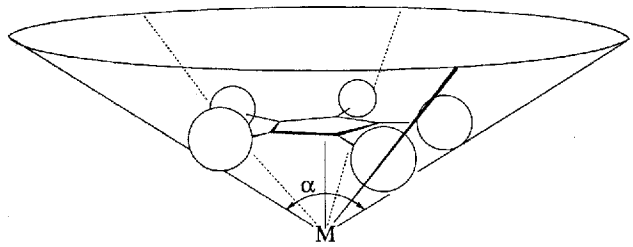

Figure 3. Illustrating the use of the (half) cone angles ($\alpha_1/2$, $\alpha_2/2$) of substituted cyclopentadienyl ligands together with the bending angle of the metallocene (β) for the calculation of the coordination gap aperture (cga)

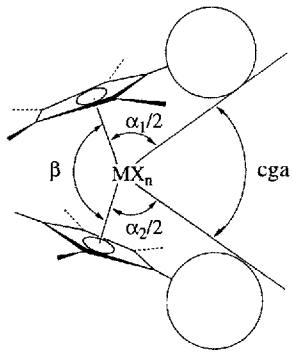

$$cga = 360° - \alpha_1/2 - \alpha_2/2 - \beta \quad (1)$$

(α_1, α_2 = cone angles for different cyclopentadienyl ligands).

Here again, the cone angle can only be determined directly for the fivefold symmetrically substituted C_5 ligands. However, from the two cone angles α and α′ of two different fivefold symmetrical ring ligands C_5R_5 and $C_5R'_5$, the

Table 1a. Cone angles (α) for $(C_5R_{5-n}R'_n)Zr$ systems[a]

R, R'	n	$C_5R_{5-n}R'_n$	cone angle[b] α / °
H	0	C_5H_5	139
Me	5	C_5Me_5	171
H, Me	4	C_5HMe_4	164
CR = P	0	P_5	152
Me, CR' = P	4	C_4Me_4P	167
^{t}Bu	5	"$C_5{}^tBu_5$"	224
H, ^{t}Bu	1	$C_5H_4{}^tBu$	156
	2	$C_5H_3{}^tBu_2$	173
	3	$C_5H_2{}^tBu_3$	190
	4	$C_5H{}^tBu_4$	207

[a] The following geometric parameters were used for the cone angle determination of the C_5R_5 ligands: d(Zr−C_5 ring centroid) = 2.20 for C_5H_5/2.22 for C_5Me_5/2.27 for C_5tBu_5, radius C_5ring = 1.18 for C_5H_5/1.20 for C_5Me_5 and C_5tBu_5, d(Zr−"P_5" ring antroid) = 2.28, radius "P_5" ring = 1.51 (here, these last two distances were taken from the X-ray structure of $(C_4Me_4P)_2ZrCl_2$[17]), C−H = 1.00, C−Me = 1.50, C−tBu = 1.52, (C−C)t_{Bu} = 1.54 Å, C_{ring}−C-$_{Me}$−H = C_{ring}−(C−C)$_{tBu}$ = 110°, van der Waals radii: C = 1.67, H = 1.32, Me = 2.00, P = 1.85 Å; note that the methyl group as a whole is assigned a van der Waals radius[18]; for C and H the intermediate value from the range given was taken (J. E. Huheey, E. A. Keiter, R. L. Keiter, *Inorganic Chemistry*, 4th ed., Harper Collins, New York, **1995**, p. 292). The bond distances were averaged from the X-ray structural data for $(C_5H_5)_2ZrCl_2$[19], $(C_5HMe_4)_2ZrCl_2$[7], $(C_4Me_4P)(C_5H_5)ZrCl_2$[7], $(C_5Me_5)(C_5H_5)$-$ZrCl_2$[20], $(C_5H_3tBu)_2ZrCl_2$[21], $(C_5H_3$-1,3-$tBu_2)_2ZrCl_2$[22], and $(C_5H_3$-1,3-$tBu_2)(C_5H_5)ZrCl_2$ [this work]. − [b] For mixed-substituted ligands the cone angle was calculated according to eq. 2.

cone angle α_i for a mixed ligand of the type $C_5R_{5-n}R'_n$ can be approximated according to equation 2[10].

$$\alpha_i = (5 - n)/5 \cdot \alpha + n/5 \cdot \alpha' \qquad (2)$$

Hence, from the cone angles of the "pure" C_5H_5, C_5Me_5, P_5[16], and the hypothetical C_5tBu_5 ligands, the cone angles of the mixed-substituted cyclopentadienyl and the phospholyl ligands can be calculated. It should be noted that the cyclopentadienyl cone angles are dependent on the metal−ligand distance. For zirconium as the apical metal the cone angles are listed in Table 1a.

To have as many structural parameters available as possible, we attempted crystallization of those *tert*-butyl substituted zirconocenes whose crystal structure was hitherto undetermined. However, crystals suitable for an X-ray structural investigation could only be obtained for $(C_5H_3$-1,3-$tBu_2)(C_5H_5)ZrCl_2$ (**10**). Figure 4 shows the molecular structure of **10** together with a stereoscopic cell plot. The two *tert*-butyl groups flank the maximum opening angle spanned by the two ring planes.

From the cone and bending angles the coordination gap apertures can now be calculated according to eq. 1. However, there is one further complication: The calculation of an average cone angle according to eq. 2, and its use in eq. 1, assumes free rotatability of the ligands. While this is true for the methyl-substituted zirconocenes, it may not be valid for the *tert*-butyl substituted analogs[24]. Molecular modeling calculations give well-formed minima for specific conformers together with barriers of rotation. To locate the minimum energy rotamers the whole hypersurface was mapped at an artificially lengthened Zr−Cp distance which just allowed for the passage of the *tert*-butyl groups upon ring rotation. The minima and their vicinities were then calculated at the realistic Zr−ring distance. It was also verified that no other minima developed upon decreasing the Zr−Cp contact. Figure 5 provides a view of the total two-dimensional energy surface and two of the four energy minima for $(C_5H_3tBu_2)_2ZrCl_2$, **11**, with respect to an independent rotation of both rings, and shows the geometries of the minimum energy rotamers. The optimized geometry in one of the minima corresponds closely to the solid state conformation as observed by an X-ray structure determination[22]. The path from one minimum to another has to involve a concerted rotation of both rings. From dynamic NMR studies of $(C_5H_4tBu)_2Zr$(s-*cis*-butadiene) and $(C_5H_2$-1,2,4-$SiMe_3)_2ZrCl_2$[28] a barrier to ring rotation of $\Delta G^{\neq}$ around 10 kcal/mol may be estimated for **9** and **11** here. When calculating the gap aperture for the *tert*-butyl zirconocenes, the hindered ring rotation and the preferential orientation of the substituents along the maximum opening

Figure 4. Molecular structure of $(C_5H_3$-1,3-$tBu_2)(C_5H_5)ZrCl_2$ (**10**) with the atomic numbering scheme and stereoscopic cell plot (PLATON-TME, 50% probability ellipsoids, and PLUTON plot, respectively)[23]. Selected distances (Å) and angles (°): Zr−Cl1 2.440(4), Zr−Cl2 2.441(3), Zr−C_{ring} 2.452(8)−2.582(6), Zr−ring(C1−C5)-centroid 2.225, Zr−ring(C6−C10)-centroid 2.173, Cl1−Zr−Cl2 93.33(7), ring-centroid−Zr−ring-centroid 129.73, ring−planes 53.99

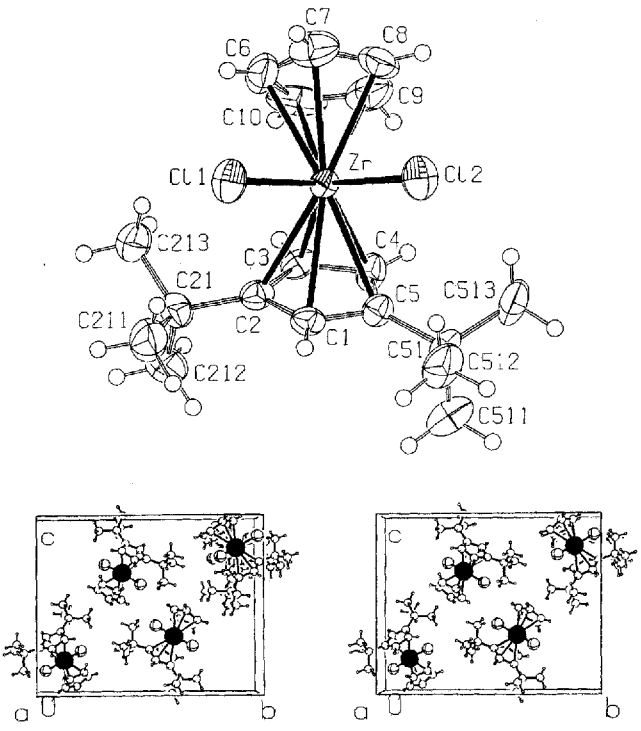

Figure 5. Energy surface for the independent rotation of both cyclopentadienyl rings in **11** at a lengthened Zr–Cp distance to allow for passage of the *tert*-butyl groups. At the actual Zr–Cp distance two of the four minima found are mapped in more detail. The minimum energy rotamers are sketched. The rotation angle, γ, corresponds here to the angle between the single C_5–H bond and the meridional centroid–Zr–centroid plane, with γ = 0° being at the minimum opening of the ring planes

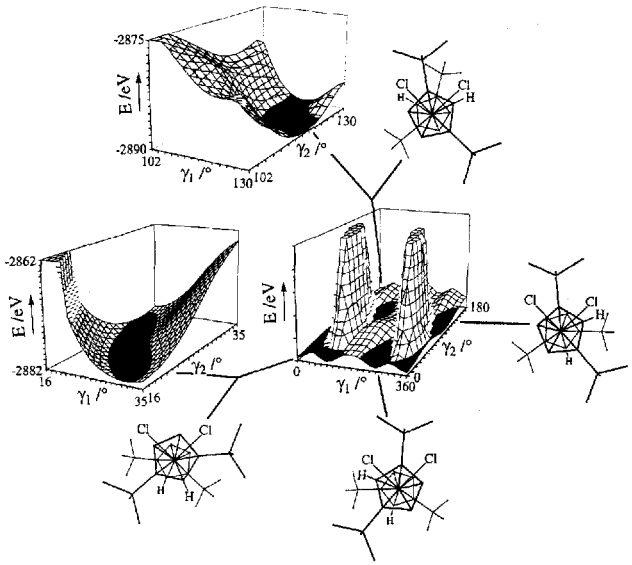

was taken into account by (surely somewhat arbitrarily) using the cone angle for the cyclopentadienyl ring with one more *tert*-butyl group. For example, for **8**, with the C_5H_4tBu ligand, the cone angle for $C_5H_3tBu_2$ was used instead, while for **11** ($C_5H_3tBu_2$ ligands) the value for $C_5H_2tBu_3$ was employed. Table 1b contains the coordination gap apertures for the zirconocenes **1**–**12**.

^{91}Zr-NMR Studies

A recent study suggests a correlation of zirconium-91 chemical shifts [$\delta(^{91}Zr)$] and line widths ($\Delta\nu_{1/2}$) with geometric parameters, most notably the tilt angle[4] (Figure 6). For a more detailed understanding of the electronic variability of the complexes involved in our study, and a possible indicator of the structural flexibility, we investigated the ^{91}Zr-NMR parameters and their dependence on alkyl substitution and coordination geometries. Table 2 lists the ^{91}Zr chemical shifts and line widths of the series of zirconocene complexes together with the experimental tilt angles, where available from X-ray crystallographic analyses.

Figure 6. Schematic representation of the tilt angle, τ (dotted line = ring normal)

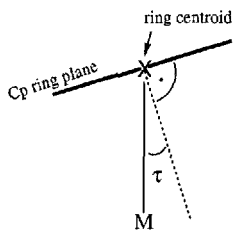

Figure 7 illustrates a fair linear dependency between the chemical shifts and the number of alkyl groups for both the methyl- and *tert*-butyl-substituted zirconocene series. When the zirconium chemical shifts are based on$(C_5H_5)_2ZrCl_2$ an increase of about 20 ppm per methyl group or 25 ppm per *tert*-butyl group is apparent. In view of the pronounced valence orbital energy dependence of bent metallocenes on the bending angle at the metal[27], and the inverse proportionality of $\delta(^{91}Zr)$ to the average excitation energy (approximated by the HOMO–LUMO gap)[25], the change in angular parameters might also explain the variation in zirconium chemical shifts[29]. To test this assumption, Figure 7 also includes plots of the zirconium chemical shifts versus the ring-centroid–zirconium–ring-centroid angle. For some of the methyl-substituted systems, including the phospholyl compounds **4** and **5**, there is a good linear dependency, but this is not the case for the *tert*-butyl substituted zirconocenes. Hence, we attribute the difference in chemical shifts mostly to the additive electronic changes induced by the ring substituents[7]. Photoelectron spectroscopy investigations on permethylated zirconocenes and ferrocenes support such an additive electronic effect on the central metal[30]. Alkyl groups are electron donating with respect to the cyclopentadienyl ring and the central metal[30,31]. Other things being equal, the difference in chemical shift between the methyl- and *tert*-butyl-substituted zirconocenes allows a comparison of the relative electron donor strength of methyl and *tert*-butyl groups. From ^{91}Zr-NMR we deduce here that a *tert*-butyl group is 1.25 times as electron donating as a methyl group. This value is somewhat lower than that suggested from photoelectron (PE) spectroscopic investigations; there the ratio was about 2[31]. The broadness of the peaks in the PE spectra leads, however, to a higher uncertainty. We note that we were unable to trace any changes in the polymerization activity (see below) to electronic differences based on the type or number of alkyl groups. Such electronic variations are apparently insignificant in comparison with the concomitant steric effects[7].

The correlation between the line width, $\Delta\nu_{1/2}$, of the zirconium NMR signal and the tilt angle, τ, shows no simple dependency (see Table 2). While within **1**–**6**–**3** or **4**–**5** or **10**–**9**–**11** the increase in line broadening agrees with the increase in the experimentally available tilt angle, a comparison between the methyl- or *tert*-butyl-substituted or phospholyl-containing zirconocenes indicates that other effects, e.g. correlation times[4], dominate the line widths. We note that even within a closely related series, the agreement between the trends in $\Delta\nu_{1/2}$ and τ might be fortuitous. The tilt angles are obtained from solid-state structural data and hence can be influenced by packing effects, while the line widths are measured in solution. Also, rings with different substituents or rings not related by crystallographic symmetry in these bent sandwich molecules will have different tilt angles, e.g. 3.6° for the C_5H_3-1,3-tBu_2 ring and 0.6° for the C_5H_5 ring in **10**, 2.0° and 0.9° for the two independent C_5H_5 rings in **1**[19a].

Table 1b. Coordination gap apertures together with bending angles at zirconium and the sum of cone angles used for the calculation in the zirconocene complexes **1**–**12**

Compound		bending angle [a] β /°	sum of half cone angles [b] $\alpha_1/2 + \alpha_2/2$ /°	coordination gap aperture [c] cga /°	Ref. to the X-ray data for β
1	$(C_5H_5)_2ZrCl_2$	129.1	139	92	19
2	$(C_5HMe_4)(C_5H_5)ZrCl_2$	132 [d]	152	76	
3	$(C_5HMe_4)_2ZrCl_2$	133.1	164	62	7
4	$(C_4Me_4P)(C_5H_5)ZrCl_2$	132.3	153	75	7
5	$(C_4Me_4P)_2ZrCl_2$	135.4	167	58	17
6	$(C_5Me_5)(C_5H_5)ZrCl_2$	130.0	155	75	20
7	$(C_5Me_5)_2ZrCl_2$	134 [d]	171	55	
			(hind. rot.) [e]	(hind. rot.) [e]	
8	$(C_5H_4{}^tBu)(C_5H_5)ZrCl_2$	130 d	156	74	
9	$(C_5H_4{}^tBu)_2ZrCl_2$	128.7	173	58	21
10	$(C_5H_3\text{-}1,3\text{-}{}^tBu_2)(C_5H_5)ZrCl_2$	129.7	164.5	66	this work
11	$(C_5H_3\text{-}1,3\text{-}{}^tBu_2)_2ZrCl_2$	129.7	190	40	22
12	$(C_5H_2\text{-}1,2,4\text{-}{}^tBu_3)(C_5H_5)ZrCl_2$	132.5 [d]	173	54.5	

[a] The ring-centroid–zirconium–ring centroid angle. For the difference in the angle between the ring normals from the zirconium center onto the ring planes, see the tilt angle in Table 2. – [b] The cone angles α are listed in Table 1a; α_1,α_2 are the cone angles for different cyclopentadienyl ligands. – [c] Calculated according to cga = 360° – $\alpha_1/2$ – $\alpha_2/2$ – β (eq. 1). – [d] Where no X-ray data was available, the bending angle was estimated from comparative ZINDO/1 calculations[7]. – [e] The hindered ring rotation and the preferential orientation of the substituents along the maximum opening was taken into account by using the cone angle for the cyclopentadienyl ring with one more *tert*-butyl group, e.g. for **12** with the $C_5H_2tBu_3$ ligand, half the cone angle for C_5HtBu_4 was entered as the value of $\alpha_1/2$.

Figure 7. Relation of ^{91}Zr chemical shifts [based on $(C_5H_5)_2ZrCl_2$] and the number of alkyl groups on the cyclopentadienyl rings (left) or the centroid–Zr–centroid bending angle, β (right) in (a) methyl- and (b) *tert*-butyl-substituted zirconocene dichloride complexes; in (b) note that there are two compounds with a total number of two *tert*-butyl groups, namely **9** and **10**. Parentheses indicate ZINDO/1 estimated bending angles

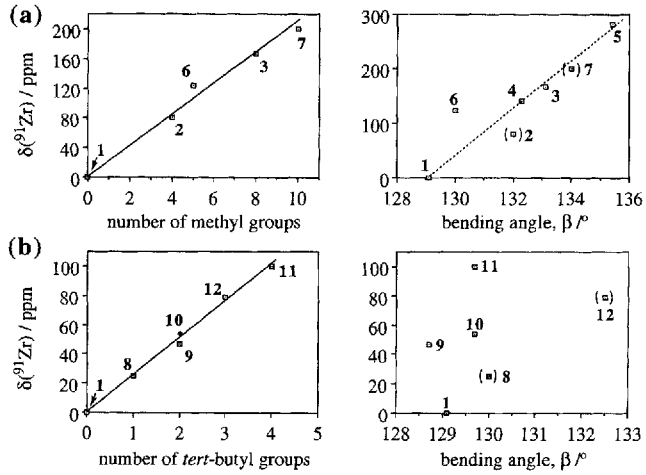

Polymerization Studies

The purpose of the polymerization experiments was to check for a correlation between the coordination gap aperture and the catalytic activity of the zirconocene complexes **1**–**12**. (Note: "Activity" in the following means an "apparent activity" since differences in activation equilibria of different complexes with MAO cannot be taken into account[7,32]). We intentionally employed only ethene as a monomer in our comparative studies, as with propene or other α-olefins the stereospecificity of the catalyst strongly affects the activity[6,9,33]. Furthermore, to give comparable catalytic activities, the polymerization conditions with ethene had to be chosen such as to avoid a diffusion-controlled process. Figure 8 illustrates this point by showing the difference in ethene uptake over time. The differential ethene consumption (dV/dt) is a direct measure of the activity at time t. In Figure 8 the activity profiles in the ethene polymerization for the two series of zirconocene complexes are given at high and low zirconocene concentration regimes. Table 3 lists the activity data. The overlapping curves of the activity profiles and the resulting similar activities for many complexes among both series at the chosen "high" zirconocene concentration of 10^{-5} mol l^{-1} are due to the rapid polyethylene precipitation under these conditions. The polymerization is truly homogeneous only at the very beginning. With the precipitation of polyethene the active complex becomes more and more embedded in the polymer matrix, which represents a transfer to a heterogeneous phase, i.e. a heterogeneous active complex form, and this leads to a diffusion-controlled reaction. The reaction rate is then controlled by the rate of diffusion of the monomer through the

Table 2. ^{91}Zr-NMR data and ring-tilt angles for the zirconocene complexes **1**–**12**

Compd.	$\delta(^{91}Zr)$[a] /ppm	$\Delta\nu_{1/2}$[b] /Hz	$\delta(^{91}Zr)$[c] /ppm	tilt angle[d] (av.) τ /°	Ref.[e]
1	–113	260	0	1.3	25
2	–22	500	81		
3	54	810	167	3.4	
4	29	1760	142	1.8	
5	170	3030	283	1.9	
6	10	340	123	1.7	
7	87	140	200		25
8	–88	1070	25		
9	–66	2800	47	2.9	4
10	–59	825	54	2.2	
11	–13	5600	100	4.4	
12	–34	880	79		

[a] Chemical shift from $(C_5H_5)_2ZrBr_2$ with $\delta = 0$; all samples measured in CH_2Cl_2/CD_2Cl_2. – [b] Frequency width at half maximum peak height. – [c] Chemical shift based on $(C_5H_5)_2ZrCl_2$. – [d] The tilt angle τ is defined as the angle between the metal–ring-centroid vector and the ring normal[26] (see Figure 6) and was calculated with the help of the PLATON program[23] from X-ray structural data as "90° minus the Zr–Cp_{cent}–ring plane angle". When the two rings are not symmetry related, two tilt angles result – one for each ring – which can be quite different. The average value is listed in the table. For the structural data, see the references given in Table 1b. – [e] References to ^{91}Zr-NMR literature data available for comparison.

polymer matrix to the enclosed active center[34] and can no longer be compared in terms of steric effects.

Eventually, a zirconium concentration of 2.5×10^{-7} mol l^{-1} together with an Al/Zr ratio of 160000:1 was found to allow comparison of the catalytic activities. The corresponding activity profiles in Figure 8 show a more constant ethene consumption. The smaller amount of polyethene produced under these conditions ensures the existence of a homogeneous phase over an extended time period. We note that with the lowering of the zirconocene concentration, the Al/Zr ratio had to be increased overproportionally to offset a higher degree of dissociation upon dilution of the catalytically active zirconocene-MAO complex[7,35].

Correlation: Polymerization Activity–Coordination Gap Aperture

The relation between the polymerization activity at low zirconium concentration and the coordination gap aperture is depicted in Figure 9, in separate plots for the methyl- and *tert*-butyl substituted zirconocenes. The methyl-cyclopentadienyl systems **2**, **3**, **6** and **7**, together with the unsubstituted zirconocene dichloride (**1**) give rise to a very good linear dependency. The points for the phospholyl systems, **4** and **5**, fall somewhat below this line, on the side of lower activity for the estimated coordination gap aperture. In other words, for the activity obtained, the calculated gap aperture is too large. As an explanation for this discrepancy we suggest the coordination of Lewis acid aluminum moieties to the Lewis base phosphorus donors, schematically shown in Figure 10 for **5**. Such an adduct would have a higher steric demand, resulting in a smaller gap aperture. (An alternative explanation, which we will not elaborate further, for the deviation from simple sterics might be the space taken up by the phosphorus "lone pairs".)

Figure 8. Activity profiles in the ethene polymerization for the two zirconocene series **1**–**7** (a) and **1**, **8**–**12** (b) activated with MAO at a zirconium concentration to molar Al/Zr ratio of 10^{-5} mol^{-1}/4000:1 (upper row) and 2.5×10^{-7} mol l^{-1}/160000:1 (lower row). In the lower row the least active complexes are omitted; for further experimental conditions see Table 3

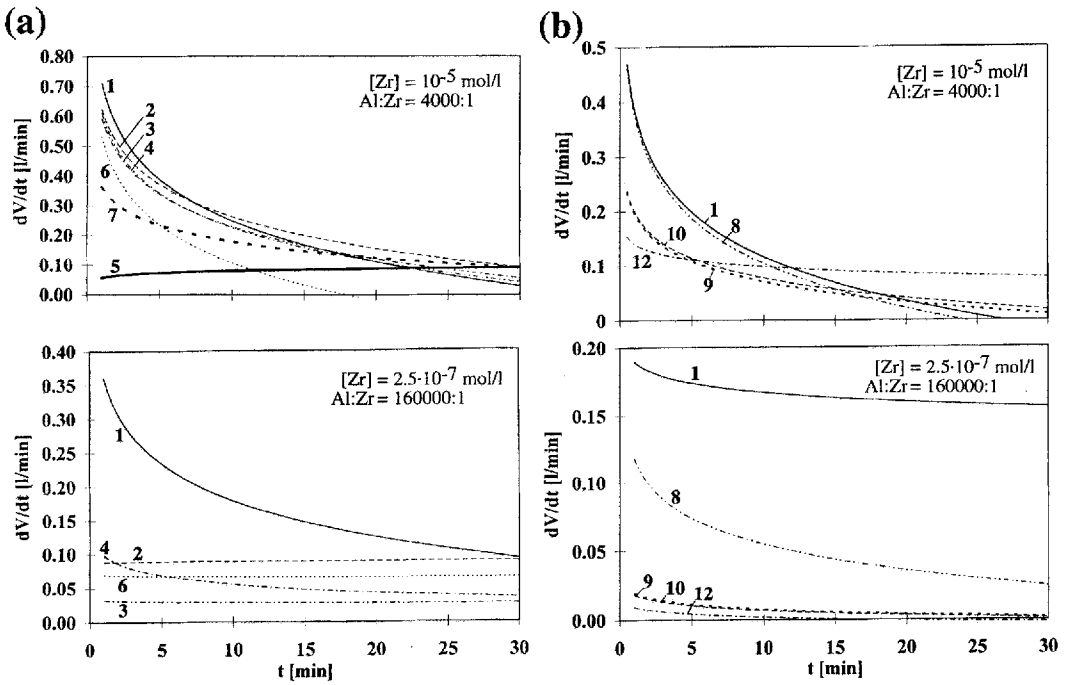

Table 3. Activity and polymer data for ethene polymerizations with zirconocene complexes **1**–**12** and MAO as a function of Zr concentration and molar Al/Zr ratio

Compd.	Activity[a]		Polymer data		
	Zr conc. conditions[b]		M_n / Q[c]	(η / M_η)[d]	M.p.[e]
	A (high)	B (low)	A	B	(B only)
1	37		49 600 / 2.4		
		756		134 000 / 2.7	
2	30		79 400 / 2.9		
		462		(10.5 / 1 210 000)	134.1
3	30		69 600 / 3.8		
		165		(8.75 / 995 000)	
4	37		63 100 / 3.5		
		262		302 000 / 2.9	
5	11		33 200 / 8.6		
		14		234 000 / 4.2	
6	30		108 000 / 2.9		
		373		(13.01 / 1 740 000)	135.6
7	19		19 500 / 4.4		
		35		(9.65 / 1 140 000)	
1	23		48 700 / 2.3		
		774		100 000 / 3.0	132.3
8	22		64 200 / 2.6		
		278		n.a.	138.0
9	9		110 000 / 4.2		
		15		n.a.	136.3
10	13		107 000 / 3.2		
		27		n.a.	138.4
11	0.2		n.d.		
		n.d.		–	
12	13		128 000 / 3.7		
		7		n.a.	134.7

[a] Activity in kg PE/(g Zr × h × bar); n.d. = not determined. – [b] T = 70 °C, ethene pressure 5 bar, 300 ml toluene, polymerization time 30 min; A: [Zr] = 10^{-5} mol l^{-1}, Al/Zr = 4000:1; B: [Zr] = 2.5 × 10^{-7} mol l^{-1}, Al/Zr = 160000:1. – [c] M_n = number average molar mass in g mol^{-1}; Q = M_w/M_n, dispersity; determined by size exclusion chromatography (SEC), except for the values in parentheses. The latter molar mass values were too high for SEC, and were approximated from the Staudinger index η. – n.a. = not available due to the insolubility of the polymer in 1,2,4-trichlorobenzene at 135 °C. – [d] η = viscosity, Staudinger index in dl g^{-1}, measured in decalin (0.1% solution) at 135 °C, M_η = viscosity averaged molar mass calculated according to the Mark-Houwing equation M_η = $(\eta/K)^{1/a}$ (for comparison purposes: M_η lies between M_n and M_w), with constants K = 51 × 10^{-3} ml g^{-1} and a = 0.706 for polyethene (low pressure) in 1,2,4-trichlorobenzene at 135 °C, in a range of M from 8 × 10^4 to 1.2 × 10^6 g mol^{-1} (see: E. P. Otocka, R. J. Roe, M. J. Hellmann, P. M. Muglia, *Macromolecules* **1971**, *4*, 507.) – [e] M.p. = melting point in °C from DSC; the results of the second scan (after one heating and cooling cycle) are reported to avoid effects of mechanical and thermal history on the samples, heating rate 10 °C min^{-1}.

Figure 9. Correlation between ethene polymerization activity and the coordination gap aperture for the methyl-substituted zirconocene series **1**–**7** (a) and the *tert*-butyl-substituted complexes **8**–**12** (b); the dashed line in (b) corresponds to the line draw in (a)

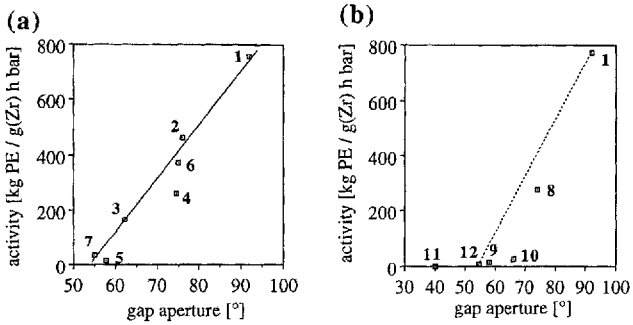

An indication of formation of these P–Al adducts in an equilibrium reaction was provided by ^{31}P NMR. At small Al/Zr ratios (below 50:1) the resonance of the phospholyl complex remains unaffected, but the ^{31}P-NMR data in Table 4 show a second phosphorus resonance starting above an Al/Zr ratio of about 50:1. From excess aluminum values above 250:1, only the second signal was observed It was ascertained that this difference in chemical shifts was not due to concentration effects. Addition of aluminum alkyls to a zirconocene dichloride complex will also lead to a reaction of the halide ligands, such as a methyl/chloride exchange, and formation of bridged Zr–Al species. Such reactions take place at relatively low Al/Zr ratios up to 25:1[36]. Since these profound changes at the zirconium center at low Al/Zr ratios are not reflected in the ^{31}P chemical shift, we suggest that the change in the ^{31}P resonance at large aluminum excess is instead due to adduct formation. Considering the magnitude and sign of the phosphorus coordination chemical shift, $\Delta(^{31}P) = \delta_{complex} - \delta_{free\ zirconocene} \approx -6.5$ ppm, similar changes in ^{31}P chemical shift on coordination have been observed in trimethylaluminum–phosphine complexes (Δ range −21 to +13 ppm). With sterically bulkier phosphines Δ was negative[37].

In view of the increased steric demand upon aluminum coordination to the phosphorus atoms one might have expected a more pronounced drop in activity for the phospholyl sytems **4** and **5**. Such a large drop is only seen in the polymerization of propene or 1-hexene. There, the activity is 1–2 orders of magnitude lower than those of the corresponding methylcyclopentadienyl zirconocenes[38]. This behavior may be explained by analogy with *ansa*-zirconocene complexes with C_5 ring substituents close to the meridional centroid–Zr–centroid plane. These are propene-inactive due to steric interaction of the substituent with the alkyl group of the olefin, but are still rather active in the polymerization of the sterically less demanding ethene[39,40].

With respect to the electronic perturbation expected upon exchanging a CH group with a phosphorus atom it might appear strange that the phospholyl complexes resemble so much their cyclopentadienyl counterparts. Ab initio calculations on model L_2TiMe^+ complexes were used to shed some light on this point. For each of the ligands C_5H_5, C_5H_4N[24,31,41] and C_5H_4P, insertion of ethene into the Ti–Me bond was studied by determining the stationary points for reactants, transition state and products. These calculations were done at the RHF level employing a small basis set, and were not intended to give quantitatively accurate results; however, they should allow a comparison of the Cp complexes with their heteroatom-substituted analogs.

For the parent Cp system, a symmetrical η^5 coordination is found as expected. Coordination of the phospholyl group is also rather symmetrical, but the pyrrolyl complex shows a significant slippage of the metal atom towards nitrogen, probably because of the concentration of negative charge in

Figure 10. Schematic drawing of the bisphospholyl zirconocene complex **5**, with one or two aluminum moieties from methylalumoxane (MAO) or trimethylaluminum (TMA) coordinated to the phosphorus donors in an equilibrium reaction. Note that reaction of the zirconocene dichloride with a methyl-aluminum species leads foremost to a reaction of the halide ligands, such as methyl/chloride exchange or abstraction, to give a zirconocenium cation; for simplicity these two ligands have been denoted here as X

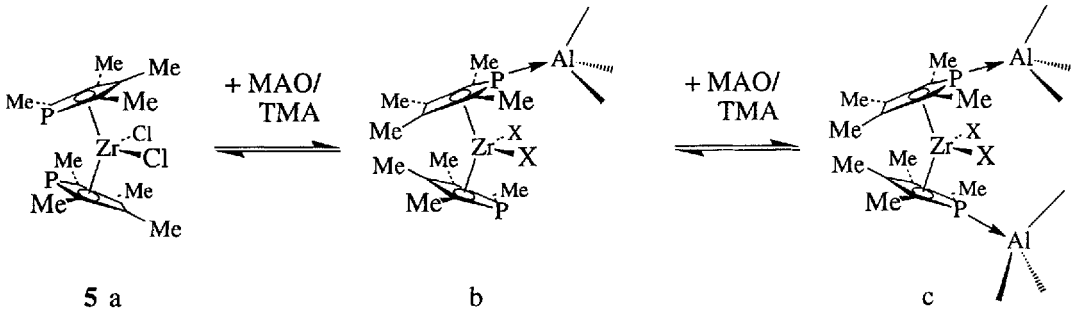

Table 4. ^{31}P-NMR data for the phospholyl-containing zirconocenes in combination with various amounts of trimethylaluminum (TMA) or methylalumoxane (MAO)

Al compd.	Al/Zr ratio[b]	Compound **4** $\delta(^{31}P)$ / ppm[c]	Compound **5**[a] (Zr conc. / mmol l^{-1})
none	–	84.51 (94)	87.17 (43)
	–		87.26 (3.5)
TMA	1:1	84.53 (90)	–
	2:1	84.52 (82)	–
	5:1	–	87.27 (4)
	10:1	84.53 (59)	87.17 (36)
	25:1	84.54 (34)	87.28 (4)
	50:1	–	87.30 (4)
	100:1		87.29/80.70[d] (4)
	200:1		87.29/80.66[d] (4)
	250:1		80.80
	500:1		80.77
	1000:1	–	80.44 (4)
			80.56 (3)
MAO	1000:1	–	80.93 (3)

[a] Note added in proof: The bis(tetramethylphospholyl)iron complex, $(C_4Me_4P)_2Fe$, was synthesized[17] and investigated by NMR spectroscopy in order to verify the P–Al adduct formation as a source of the shift of the P resonance upon addition of TMA and to exclude the influence of side reactions at the Zr–Cl bonds. The ^{31}P resonance of the pure iron complex appeared at −60.37 ppm, with TMA at Al/Fe ratios of 50, 100 and 150:1, the signal shifted to −54.7 ppm (same concentration, toluene solution). – [b] Molar ratio. – [c] Bruker ARX 200, 80.0 MHz for ^{31}P, samples in toluene/[D_8]toluene. TMA or MAO was added as a toluene solution to the zirconocene solutions in [D_8]toluene. – [d] The intensity ratio of the two signals is about 1:5.

Figure 11. Projections of Ti atom on ligand ring for Cp_2TiMe^+ (A), $(C_5H_4P)_2TiMe^+$ (B) and $(C_5H_4N)_2TiMe^+$ (C); bond lengths in A

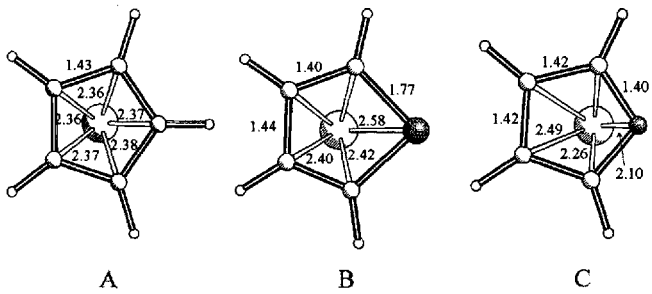

Table 5. Energies relative to separated reactants (kcal/mol) for insertion of ethene in L_2TiMe^+[a]

L	Complex	T.S.[b]	Product
C_5H_5	–3.8	14.6	–21.6
C_5H_4P	–3.1	15.6	–22.2
C_5H_4N	–4.0	10.9	–23.0

[a] Barriers calculated at higher levels than RHF and with better basis sets tend to be much lower, sometimes even close to zero. Thus, our values should not be compared directly to any experimental values. However, comparison of the values for the three ligands should give a reasonable indication of the electronic effects of introducing a heteroatom in a metallocene. – [b] T.S. = transition state.

that region. Projections of the metal atom onto the ring plane are shown in Figure 11.

The metal–ring interaction does not change significantly during olefin insertion: the Cp and phospholyl ligands remain symmetrically η^5-coordinated, and the pyrrolyl group retains its slipped coordination mode. This is reflected in the olefin insertion barriers (Table 5): the Cp and phosphonyl complexes have nearly the same barriers, whereas the slipped pyrrolyl complex is less crowded and has a somewhat lower barrier.

Thus, it appears that the phospholyl group is indeed electronically very similar to a Cp group, both in ground-state geometry and in its influence on olefin insertion reactions. The reason for this must be the similar electronegativities of carbon (2.5) and phosphorus (2.1): substitution by the more electronegative nitrogen atom (3.0) results in significant changes in structure and reactivity. Of course, one cannot expect a perfect parallel between Cp and phospholyl chemistry: the phospholyl group has a reactive lone pair which introduces complications not found for the more inert Cp group. In addition, coordination of e.g. Al to P

should have some influence on both steric and electronic properties of the complex.

The relation between the polymerization activity and the gap aperture for the *tert*-butyl zirconocenes (Figure 9b) reflects the more complicated approximation of the gap aperture because of the hindered ring rotation (see above). There is no linear dependency for all data points. When comparing the data points to the relation obtained from the methyl-substituted series (dashed line in Figure 9b), it could be argued that the estimated gap aperture for **8** and **10** is still too large, if one assumes the same relation irrespective of the kind of substituent. Furthermore, it is evident that a minimum gap aperture of about 50° is necessary for a polymerization activity. At a gap aperture below 50° only very low activities are observed (compound **11**). From this, the aforementioned deviation of **8** and **10** may be attributed to the presence of rotamers having the *tert*-butyl group(s) pointing along the maximum opening where the polymerization reaction takes place, so that the actual gap aperture for this rotamer becomes smaller than 50°. As a *tert*-butyl group in this position blocks the path of the C–C bond-forming reaction, the respective rotamer would be inactive, hence lowering the number of active species.

Aside from the activity–gap-aperture correlation further remarks concerning the catalyst activity and the polymer parameters can be made:

(i) The polymer dispersity (Q, Table 3) is rather narrow, as expected for metallocene catalysts. The slight increase of Q to 3–4, from the theoretical value of 2 for a Schulz-Flory distribution, is explained by the polyethene precipitation and subsequent heterogenation of the reaction mixture. Nevertheless, the even broader dispersity of Q= 8.6 for the bisphospholyl complex **5** is remarkable, and is due to a bimodal molar mass distribution as shown in Figure 12. Similar bimodal molar mass distributions with even broader dispersities of $Q > 10$ were observed for the bispentamethyl complex **7** at zirconium concentrations below 5.0×10^{-6} mol/l and Al/Zr ⩾ 8000:1. Therefore, at least two types of reactive centers must be present. We suggest that the complexes with the more bulky tetramethyl- and pentamethyl-ligands are more prone to ligand loss, with the half-sandwich complex still continuing to be an active polymerization catalyst[42].

Figure 12. Bimodal molar mass distribution of polyethene obtained with the bisphospholyl zirconocene **5**

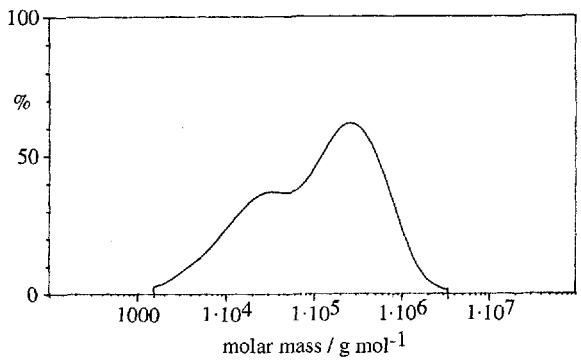

(ii) In our series of comparisons, the polyethene properties are affected most dramatically by a variation in transition metal concentration such that a decrease in zirconium concentration gives rise to a large increase in molar mass (cf. Table 3) to the extent that the polyethene is no longer soluble for SEC measurements. Such substantial molar mass increases upon a decrease in zirconocene concentration have been observed before[35,43]. Two possible explanations are discussed for this not fully understood phenomenon[39]: (a) a dilution effect favoring the active complex form over the inactive precursor or dormant species and hence the rate of chain propagation (k_P) over that of chain termination (k_T). It is thereby assumed that chain terminations arise predominantly from "dormant", i.e. temporarily inactive, zirconocene species. (b) A bimolecular chain-transfer mechanism involving the active complex and a second (active or inactive) zirconocene species is proposed by Kaminsky et al.[43]. A decrease in zirconocene concentration would then reduce the rate of the termination reaction, k_T. The mean degree of polymerization, P_n, which is proportional to the number average molecular weight M_n, is given by the ratio of the growth rate to the rate of transfer, $M_n \sim P_n \approx k_P/k_T$[39].

(iii) Within the *tert*-butyl substituted zirconocene series, the more sterically demanding complexes **9**, **11** and **12** showed rather low polymerization activities. Since it might have been possible that the more sterically demanding complexes were activated more slowly, we carried out a brief investigation of the influence of activation or ageing times, i.e. the time the zirconocene dichloride and MAO were allowed to react before pressurizing with ethene. The results are summarized in Table 6. Normally, the activation time was 10 min. Extending this time to 24 h led to considerable increase in activity for unsubstituted zirconocene dichloride (**1**) and the mono *tert*-butyl substituted complex **8**. For complexes with two *tert*-butyl groups, **9** and **10**, the rise in activity became very small, while for the tris-*tert*-butyl

Table 6. Influence of activation times on the polymerization activity of zirconocene/MAO systems

Compd.	Activity[b] after activation time[a]		
	10 min	3 h	24 h
1	23	49	57
8	22	–	37
9	9	9	11
10	13	–	15
12	13	–	5

[a] Conditions of activation: In the case of an activation time of 10 min, the reactants were dissolved in 300 ml of toluene, previously thermostatted at 70 °C. For the 3 h and 24 h activation times, three-quarters of the MAO solution was added to the zirconocene dissolved in a small amount of toluene (giving Al/Zr ≈ 3000:1), and the mixture was allowed to stand for 3 h or 24 h, respectively. The rest of the required MAO solution (1/4) had been previously added to the 300 ml portion of toluene for purification purposes. – [b] Activity in kg PE/(g Zr × h × bar). Polymerization conditions: T = 70 °C, ethene pressure 5 bar, 300 ml toluene, polymerization time 30 min; [Zr] = 10^{-5} mol l^{-1}, Al/Zr = 4000:1.

substituted zirconocene **12** the activity was even decreased. An increase of activity with ageing (5 to 60 min) has been reported for $(C_5H_5)_2ZrCl_2$/MAO+TMA in ethene polymerization, yet a decrease was seen with $(C_5H_5)_2ZrCl_2$/MAO in the polymerization of propene[44].

Conclusions

In the ethene polymerization with non-*ansa* alkyl-substituted cyclopentadienyl and phospholyl zirconocene/MAO systems the catalyst activity under comparable, mostly homogeneous conditions is a function of steric factors. The order of activity follows the order of steric demand. This steric demand can be quantified through the coordination gap aperture, which was in turn obtained through the ring cone angle and the zirconium bending angle. In the case of not freely rotatable rings, such as the *tert*-butyl substituted ligands, the influence of specific rotamers must be considered to account for the activity–gap aperture correlation.

The phospholyl zirconium compounds give Lewis acid/base adducts with aluminum species (MAO or TMA) at high Al/Zr ratios, in an apparent equilibrium reaction, as shown by ^{31}P NMR. Alteration of the steric situation through this adduct formation is seen in the activity–gap aperture correlation.

Zirconium-91 NMR studies show a fairly linear additive electronic effect of the alkyl groups on the cyclopentadienyl ring or of the phosphorus on the central metal. From this, the relative electronic donor effect of a *tert*-butyl group versus a methyl substituent is estimated to be 1.25. No influence of these electronic effects can be seen, however, in the polymerization activity.

This work was supported by the *Deutsche Forschungsgemeinschaft* through grant Ja466/3-1, the *Fonds der Chemischen Industrie*, and the *Gesellschaft der Freunde der TU Berlin*. The *Polyolefin Division of BASF AG*, Ludwigshafen is thanked for the donation of ethene, MAO and the analyses of polymers, Prof. *H. Schumann* for his continuous support, and Dr. *D. M. Proserpio* (University of Milano) for a copy of the CACAO program. We are grateful to Mrs. *A. Müller* for the DSC measurements.

Experimental

Instruments: CHN analysis, Perkin-Elmer Series II CHNS/O Analyzer 2400. – NMR spectroscopy, Bruker ARX 200 or ARX 400 (^1H and ^{13}C chemical shifts are referenced to TMS via the solvent signal, ^{31}P to external 85% H_3PO_4, ^{91}Zr NMR spectra were measured at ambient temperature against Cp_2ZrCl_2 as external reference [dissolved in an 8:1 mixture of CH_2Cl_2/CD_2Cl_2] with $\delta = -113$ ppm from Cp_2ZrBr_2[25]). – Mass spectrometry, Varian MAT 311A/AMD (mass spectrometry peaks given refer to the most abundant isotope combination, which contains ^{90}Zr, ^{35}Cl, except when two chlorines are present. In this case, the peak arising from $^{90}Zr^{35}Cl^{37}Cl$ and $^{92}Zr^{35}Cl_2$ is of maximum intensity, as proven by an isotope simulation, but the $^{90}Zr^{35}Cl_2$ peak is cited to match the fragment losses). – Size exclusion chromatography (SEC, GPC), Waters 150 chromatography at 135°C, solvent 1,2,4-trichlorobenzene. – DSC, Perkin-Elmer Series 7 Thermal Analysis System.

Materials: All complexes were purified by sublimation and the purity was checked by elemental analysis, NMR spectroscopy and mass spectrometry. The analytical data matched the literature values. Analytical data obtained by us and not previously cited in the literature are given below. $(C_5H_5)_2ZrCl_2$ was purchased from Merck and used without further purification. Methylalumoxane (MAO) was obtained from Witco (Bergkamen, Germany) as a 10 wt.-%-toluene solution (4.92 wt.-% aluminum, density ≈ 0.9 g/ml, average molecular weight of the MAO oligomers 900–1100 g/mol). Solvents were dried over sodium metal (toluene and benzene), sodium benzophenone ketyl (pentane and diethyl ether) or potassium metal (hexane and THF), followed by distillation and storage under argon. Ethene (BASF AG) was polymerization grade and used without further purification. All experiments were carried out under argon using standard Schlenk techniques. The known zirconocene dichlorides were prepared according to literature procedures, or slight modifications thereof, as given below: *(C5HMe4)(C5H5)ZrCl2* **(2)**[7], *(C5HMe4)2ZrCl2* **(3)**[7,45], *(C4Me4P)(C5H5)ZrCl2* **(4)**[7], *(C4Me4P)2ZrCl2* **(5)**[7,18], *(C5Me5)(C5H5)ZrCl2* **(6)**[7,46], *(C5Me5)2ZrCl2* **(7)**][7,47], *(C5H4tBu)(C5H5)ZrCl2* **(8)**[48]: ^1H NMR (C_6D_6): δ = 1.23 (s, *t*Bu), 5.69 (t, $^3J(H,H)$ = 2.7 Hz, C_5-2,3-H), 5.95 (s, C_5H_5), 6.01 (t, $^3J(H,H)$ = 2.7 Hz, C_5-2,3-H). – ^{13}C NMR (C_6D_6): δ = 31.26 (CH_3C), 33.37 (CH_3C), 112.54, 115.34 (C_5-C-2,3), 115.69 (C_5H_5), 144.15 (C_5-C-1).

(C5H4tBu)2ZrCl2 **(9)**[49]: ^1H NMR (C_6D_6): δ = 1.29 (s, *t*Bu), 5.76 (t, $^3J(H,H)$ = 2.7 Hz, C_5-2,3-H), 6.08 (t, $^3J(H,H)$ = 2.7 Hz, C_5-2,3-H). – ^{13}C NMR (C_6D_6): δ = 31.34 (CH_3C), 33.49 (CH_3C), 111.71, 115.99 (C_5-C-2,3), 143.74 (C_5-C-1). – MS (EI, 70 eV, 80°C): *m/z* (%) = 402 (21, $[M]^{+\bullet}$), 387 (33, $[M - CH_3]^+$), 367 (3, $[M - Cl]^+$), 351 (100, $[M - HCl - CH_3]^+$), 281 (28, $[M - C_5H_4tBu]^+ = [(C_5H_4tBu)ZrCl_2]^+$), 265 (22, $[(C_5H_4tBu)ZrCl_2 - CH_4]^+$), 245 (16, $[(C_5H_4tBu)ZrCl_2 - HCl]^+$), 229 (51, $[(C_5H_4tBu)ZrCl_2 - HCl - CH_4]^+$).

(C5H3-1,3-tBu2)(C5H5)ZrCl2 **(10)**: A solution of 0.77 g (4.31 mmol) of 1,3-$C_5H_4tBu_2$[50] in 10 ml of toluene was reacted with an equimolar amount of *n*-BuLi (1.6 M in hexane). After stirring for 30 min, the light-yellow solution was added dropwise to a slurry of $C_5H_5ZrCl_3(dme)$[51] in 10 ml of toluene. When the addition was complete, the mixture was refluxed for 3 h. The orange toluene solution was decanted from some precipitate and the solvent was removed in vacuo. The off-white residue was then sublimed at 130–140°C/0.1 Torr to give the product as snow-white fine needles (yield 0.7 g, 40%, not optimized). Crystals suitable for X-ray structure analysis were obtained upon slow solvent evaporation from a dichloromethane solution at 2°C. – ^1H NMR (C_6D_6): δ = 1.17 (s, *t*Bu), 5.94 (d, $^4J(H,H)$ = 2.6 Hz, C_5-4,5-H), 6.12 (s, C_5H_5), 6.18 (t, $^4J(H,H)$ = 2.6 Hz, C_5-2-H); (CD_2Cl_2): δ = 1.27 (s, *t*Bu), 6.37 (m, C_5-2,4,5-H), 6.48 (s, C_5H_5). – ^{13}C NMR (C_6D_6): δ = 31.30 (CH_3C), 33.84 (CH_3C), 112.32 (C_5-C-2), 112.42 (C_5-C-4,5), 115.95 (C_5H_5), 144.05 (C_5-C-1,3). – MS (EI, 70 eV, 100°C): *m/z* (%) = 402 (35, $[M]^{+\bullet}$), 387 (41, $[M - CH_3]^+$), 367 (6, $[M - Cl]^+$), 351 (100, $[M - HCl - CH_3]^+$), 337 {73, $[M - C_5H_5]^+ = [(C_5H_3tBu_2)ZrCl_2]^+$}, 321 {18, $[(C_5H_3tBu_2)ZrCl_2 - CH_4]^+$}, 301 {12, $[(C_5H_3tBu_2)ZrCl_2 - HCl]^+$}, 285 {17, $[(C_5H_3tBu_2)ZrCl_2 - HCl - CH_4]^+$}, 269 {22, $[(C_5H_3tBu_2)ZrCl_2 - HCl - 2\ CH_4]^+$}, 225 (16, $[C_5H_5ZrCl_2]^+$), 57 (23, $[tBu]^{+\bullet}$), 41 (25, $[tBu - CH_4]^{+\bullet}$). – $C_{18}H_{26}ZrCl_2$ (404.53): calcd. C 53.44, H 6.48; found C 53.37, H 6.60.

(C5H3-1,3-tBu2)2ZrCl2 **(11)**[53]: ^1H NMR (C_6D_6): δ = 1.32 (s, *t*Bu), 5.83 [d, $^4J(H,H)$ = 2.6 Hz, C_5-4,5-H], 6.63 [t, $^4J(H,H)$ = 2.6 Hz, C_5-2-H]. – ^{13}C NMR (C_6D_6): δ = 31.15 (CH_3C), 34.12

(CH_3C), 105.38 (C_5-C-4,5), 122.79 (C_5-C-2), 144.29 (C_5-C-1,3). – MS (EI, 70 eV, 120°C): *m/z* (%) = 514 (12, $[M]^{+\bullet}$), 499 (2, $[M - CH_3]^+$), 479 (2, $[M - Cl]^+$), 463 (2, $[M - HCl - CH_3]^{+\bullet}$), 337 {97, $[M - C_5H_3tBu_2]^+ = [(C_5H_3tBu_2)ZrCl_2]^+$}, 321 {13, $[(C_5H_3tBu_2)ZrCl_2 - CH_4]^+$}, 305 {6, $[(C_5H_3tBu_2)ZrCl_2 - 2\ CH_4]^+$}, 301 {5, $[(C_5H_3tBu_2)ZrCl_2 - HCl]^+$}, 285 {12, $[(C_5H_3tBu_2)ZrCl_2 - HCl - CH_4]^+$}, 269 {15, $[(C_5H_3tBu_2)ZrCl_2 - HCl - 2\ CH_4]^+$}.

(C_5H_2-1,2,4-tBu_3)(C_5H_5)$ZrCl_2$ (**12**)[52]: MS (EI, 70 eV, 120°C): *m/z* (%) = 458 (30, $[M]^{+\bullet}$), 443 (19, $[M - CH_3]^+$), 423 (4, $[M - Cl]^+$), 407 (49, $[M - HCl - CH_3]^{+\bullet}$), 393 {100, $[M - C_5H_5]^+ = [(C_5H_2tBu_3)ZrCl_2]^+$}, 377 {11, $[(C_5H_2tBu_3)ZrCl_2 - CH_4]^+$}, 341 {9, $[(C_5H_2tBu_3)ZrCl_2 - CH_4 - HCl]^+$}, 325 {16, $[(C_5H_2tBu_3)ZrCl_2 - HCl - 2\ CH_4]^+$}, 309 {16, $[(C_5H_2tBu_3)ZrCl_2 - HCl - 3\ CH_4]^+$}, 225 (11, $[M - C_5H_2tBu_3]^+ = [C_5H_5ZrCl_2]^+$), 57 (83, $[tBu]^{+\bullet}$), 41 (35, $[tBu - CH_4]^{+\bullet}$).

Polymerizations: Polymerization reactions were carried out in a 1 l Büchi-glass autoclave, thermostatted to 70°C and charged with 300 ml toluene, MAO and the transition metal complex. The catalyst amount, concentration and Al/Zr ratio are specified in the respective tables. After a preactivation time of 10 min the autoclave was pressurized with 5 bar ethene and after 30 min the reaction was stopped by draining the toluene/polyethene slurry into an acidified (HCl) water/methanol mixture. It was then stirred for 4 h to achieve complete catalyst-MAO decomposition and dissolution within the polymer matrix. The polymer was separated by filtration, washed with hexane and dried at 80°C. To ensure reproducibility, polymerizations were carried out at least twice with each zirconium complex and a series of polymerization runs was performed with charges from the same toluene and MAO batch. To avoid ageing effects of MAO[54], a series of comparative polymerizations was run within a week.

Modeling Calculations: The semi-empirical ZINDO/1 geometry optimizations[55] for the estimation of angular structural data were performed with the program HyperChem (Version 3.0, Autodesk Inc., Sausolito, CA 94965, USA).

For the potential energy calculations of the ring rotations the computations were performed within the extended-Hückel formalism[56] with weighted H_{ij}'s[57] and the use of the CACAO program (Version 4.0)[58]. An extended-Hückel molecular orbital (EHMO) program was used because it provided a dummy atom topology for the ring centroid and thereby allowed for a controlled rotation of the cyclopentadienyl rings. The atomic parameters for the elements involved in these EHMO calculations were as follows (H_{ii}, ζ): Zr 5*s*, −9.87 eV, 1.817; 5*p*, −6.76 eV, 1.776; 4*d*, −11.18 eV, 3.835, 1.505 (coefficients for double-ζ expansion: 0.6224, 0.5782)[59]; Cl 3*s*, −26.30 eV, 2.183; 3*p*, −14.20 eV, 1.733[60]; C 2*s*, −21.4 eV, 1.625; 2*p*, −11.4 eV, 1.625[56]; H 1*s*, −13.6 eV, 1.3[56]. Geometrical parameters were fixed as follows: Zr−C = 2.51, Zr−Cl = 2.44, $(C-C)_{Cp}$ = 1.42, C−H = 1.00, $(C-C)_{tBu}$ = 1.50, Cl−Zr−Cl = 98°.

The ab initio calculations were of the all-electron closed-shell or open-shell Restricted Hartree-Fock type[61], and were carried out using the GAMESS program[62] on IBM RS/6000 and Silicon Graphics Crimson workstations. For the ligands we used the STO-3G minimal basis set[63]; the "reacting" organic fragments (methyl, olefin) were described with the 3-21G split-valence basis set.[64] For metal atom (Ti) we used the Dunning split-valence basis[65]. Some geometric constraints (described below) were used for the ligands, but the remainder of the molecule was always fully optimized, without any symmetry restrictions.

In optimizations of cyclopentadienyl compounds, local D_{5h} symmetry was enforced for each ring, and equal C−C and C−H bond lengths for the two rings. However, the rings were allowed to "breathe" and to move in space as rigid bodies, which allows ring slippage and asymmetry between the two metal−ring interactions. We never saw any evidence of such deformations in our optimized geometries. As a check, we also did a full, unconstrained geometry optimization on Cp_2TiMe^+. This still produced symmetrical η^5 Cp−Ti bonding; the only difference with the constrained structure was a small amount of bending of the ring hydrogens out of the ring plane, away from the metal atom. In calculations involving the pyrrolyl and phospholyl ligands, we first did a full geometry optimization on the $L_2TiCH_3^+$ derivatives. The ligands were then averaged to local C_{2v} symmetry, and further derivatives were optimized by refining the ligands as rigid bodies. The energy difference between the fully optimized and the constrained structures is 2−3 kcal/mol, and the geometrical differences are very small. Table 7 gives the calculated total energies at optimized geometries.

Table 7. Total energies (a.u.) for insertion of ethene into L_2TiMe^+

L	L_2TiMe^+	$L_2TiMe(C_2H_4)^+$	$L_2Ti(Me..C_2H_4)^+$	$L_2Ti^nPr^+$
C_5H_5	−1267.39455	−1345.00156	−1344.97215	−1345.02995
C_5H_4P	−1865.34475	−1942.95068	−1942.92091	−1942.98110
C_5H_4N	−1298.90182	−1376.50916	−1376.48534	−1376.53945

(C_2H_4: −77.60099 a.u.).

X-ray Structure Determination of 10

Crystal Data: Molecular formula $C_{18}H_{26}Cl_2Zr$, formular weight 404.51 g/mol, a = 6.631(3), b = 18.843(9), c = 15.265(5) Å, β = 91.3°, Z = 4, d_{calc} = 1.409 g/cm^3, monoclinic, $P2_1/n$ (No. 14). – *Data Collection:* STOE four-circle diffractometer, Mo-K_α radiation (λ = 0.71069 Å), graphite monochromator, crystal size 0.40 × 0.10 × 0.05 mm^3, 293 K, ω-scan, $4 < 2\Theta < 50°$, $-1 \leq h \leq 7$, $-22 \leq k \leq 22$, $-18 \leq l \leq 17$, 7303 reflections measured, 3347 independent, μ(Mo-K_α) 8.49 cm^{-1}, no absorption correction. – *Structural Analysis and Refinement:* Structure solution was performed by direct methods (SHELXS-86[66]). Refinement: Full-matrix least-squares on F^2 (SHELXL-93[66]); all atomic positions except those for the *tert*-butyl hydrogens were found and refined (non-hydrogen atoms with anisotropic temperature factors), 218 refined parameters, final *R1* = 0.0683, *wR2* = 0.1141 for 1896 reflections with $I > 2\sigma(I)$, goodness-of-fit on F^2 = 1.023[67].

☆ Dedicated to Prof. Dr. *Karl-Heinz Reichert* on the occasion of his 60th birthday.

[1] *Ziegler Catalysts* (G. Fink, R. Mühlhaupt, H. H. Brintzinger, Eds.), Springer Verlag, Berlin **1995**.

[2] For notes concerning the industrial application, see e.g.: *Chemical & Engineering News* **1995**, *October 30*, p. 10; *September 18*, p. 17; *September 11*, p. 15–20; *May 22*, p. 34–38. *May 1*, p. 7–8. R. Mühlhaupt, B. Rieger, *Chimia* **1995**, *49*, 486–491.

[3] For recent work on metallocene catalysis, see for example: R. H. Grubbs, G. W. Coates, *Acc. Chem. Res.* **1996**, *29*, 85–93. J. P. Mitchell, S. Hajela, S. K. Brookhart, K. I. Hardcastle, L. M. Henling, J. E. Bercaw, *J. Am. Chem. Soc.* **1996**, *118*, 1045–1053. K. Patsidis, H. G. Alt, W. Milius, S. J. Palackal, *J. Organomet. Chem.* **1996**, *509*, 63–71. M. Arnold, O. Henschke, J. Knorr, *Macromol. Chem. Phys.* **1996**, *197*, 563–573. L. Resconi, R. L. Jones, A. L. Rheingold, G. P. A. Yap, *Organometallics* **1996**, *15*, 998–1005. T. Yoshida, N. Koga, K. Morokuma, *Organometallics* **1996**, *15*, 766–777. J. Koivumäki, *Polym. Bull.* **1996**, *36*, 7–12. C. Psiorz, G. Erker, R. Fröhlich, M. Grehl, *Chem. Ber.* **1995**, *128*, 357–364.

[4] M. Bühl, G. Hopp, W. von Philipsborn, S. Beck, M.-H. Prosenc, U. Rief, H.-H. Brintzinger, *Organometallics* **1996**, *15*, 778–785.

[5] P. C. Möhring, N. J. Coville, *J. Organomet. Chem.* **1994**, *479*, 1–29.
[6] C. Janiak, K. C. H. Lange, P. Marquardt, *Macromol. Rapid Commun.* **1995**, *16*, 643–650.
[7] C. Janiak, U. Versteeg, K. C. H. Lange, R. Weimann, E. Hahn, *J. Organomet. Chem.* **1995**, *501*, 219–234.
[8] J. Tian, B. Huang, *Macromol. Rapid Commun.* **1994**, *15*, 923–928.
[9] W. Kaminsky, R. Engehausen, K. Zoumis, W. Spaleck, R. Rohrmann, *Macromol. Chem.* **1992**, *193*, 1643–1651.
[10] D. White, N. J. Coville, *Adv. Organomet. Chem.* **1994**, *36*, 95–158.
[11] P. C. Möhring, N. J. Coville, *J. Mol. Catal.* **1992**, *77*, 41–50.
[12] P. C. Möhring, N. Vlachakis, N. E. Grimmer, N. J. Coville, *J. Organomet. Chem.* **1994**, *483*, 159–166.
[13] P. Burger, K. Hortmann, H.-H. Brintzinger, *Macromol. Chem. Macromol. Symp.* **1993**, *66*, 127–140. K. Hortmann, H.-H. Brintzinger, *New J. Chem.* **1992**, *16*, 51–55.
[14] C. Janiak, H. Schumann, *Adv. Organomet. Chem.* **1991**, *33*, 291–393. J. Okuda, *Top. Curr. Chem.* **1991**, *160*, 97–145.
[15] N. J. Coville, M. S. Loonat, D. White, D. Carlton, *Organometallics* **1992**, *11*, 1082–1090.
[16] Cyclo-P_5 is not hypothetical but can be stabilized in the coordination sphere of transition metals; see O. J. Scherer, *Comments Inorg. Chem.* **1987**, *6*, 1–22. M. Baudler, S. Akpapoglou, D. Ouzounis, F. Wasgestian, B. Meinigke, H. Budzikiewicz, H. Münster, *Angew. Chem. Int. Ed. Engl.* **1988**, *27*, 280; *Angew. Chem.* **1988**, *100*, 288; M. Baudler, T. Etzbach, *Angew. Chem. Int. Ed. Engl.* **1991**, *30*, 580; *Angew. Chem.* **1991**, *103*, 580.
[17] F. Nief, F. Mathey, L. Ricard, F. Robert, *Organometallics* **1988**, *7*, 921–926.
[18] L. Pauling, *The Nature of the Chemical Bond*, 3rd ed., Cornell University Press, Ithaca, N.Y., **1960**, p. 260–261.
[19] [19a] K. Prout, T. S. Cameron, R. A. Forder, S. R. Critchley, B. Denton, G. V. Rees, *Acta Crystallogr., Sect. B* **1974**, *30*, 2290–2304. – [19b] I. A. Ronova, N. V. Alekseev, N. I. Gapotchenko, Yu. T. Struchkov, *Zh. Strukt. Khim.* **1970**, *11*, 584–589.
[20] R. D. Rogers, M. M. Benning, L. K. Kurihara, K. J. Moriarty, M. D. Rausch, *J. Organomet. Chem.* **1985**, *293*, 51–60.
[21] R. A. Howie, G. P. McQuillan, D. W. Thompson, G. A. Lock, *J. Organomet. Chem.* **1986**, *303*, 213–220.
[22] U. Böhme, H. Langhof, *Z. Krist.* **1993**, *206*, 281–283.
[23] A. L. Spek, *PLATON-93, PLUTON-92 graphics program;* University of Utrecht, The Netherlands. A. L. Spek, *Acta Crystallogr., Sect. A* **1990**, *46*, C34.
[24] N. Kuhn, G. Henkel, J. Kreutzberg, S. Stubenrauch, C. Janiak, *J. Organomet. Chem.* **1993**, *456*, 97–106, and references therein.
[25] R. Benn, A. Rufinska, *Angew. Chem. Int. Ed. Engl.* **1986**, *25*, 861–891.
[26] C. G. Howard, G. S. Girolami, G. Wilkinson, M. Thornton-Pett, M. B. Hursthouse, *J. Am. Chem. Soc.* **1984**, *106*, 2033–2040.
[27] J. W. Lauher, R. Hoffmann, *J. Am. Chem. Soc.* **1976**, *98*, 1729–1742.
[28] G. Erker, T. Mühlenbernd, A. Rufinska, R. Benn, *Chem. Ber.* **1987**, *120*, 507–519. C. H. Winter, D. A. Dobbs, X.-X. Zhou, *J. Organomet. Chem.* **1991**, *403*, 145–151.
[29] U. Böhme, K. H. Thiele, A. Rufinska, *Z. anorg. allg. Chem.* **1994**, *620*, 1455–1462.
[30] P. G. Gassman, D. W. Macomber, J. W. Hershberger, *Organometallics* **1983**, *2*, 1470–1472. P. G. Gassman, M. R. Callstrom, *J. Am. Chem. Soc.* **1987**, *109*, 7875–7876. C. Cauletti, J. C. Green, M. R. Kelly, P. Powell, J. v. Tilborg, J. Robbins, J. Smart, *J. Electr. Spectr. Rel. Phenom.* **1980**, *19*, 327–353. S. Evans, M. L. H. Green, B. Jewitt, A. F. Orchard, C. F. Pygall, *J. Chem. Soc., Faraday Trans. II* **1972**, *68*, 1847–1865.
[31] C. Janiak, N. Kuhn, R. Gleiter, *J. Organomet. Chem.* **1994**, *475*, 223–227.
[32] D. Fischer, S. Jüngling, R. Mühlhaupt, *Makromol. Chem., Macromol. Symp.* **1993**, *66*, 191–202. D. Fischer, Ph. D. Thesis, University of Freiburg, Germany, **1992**. D. Fischer, R. Mühlhaupt, *J. Organomet. Chem.* **991**, *417*, C7–C11.
[33] T. Uozumi, K. Soga, *Makromol. Chem.* **1992**, *193*, 823–831.
[34] G. Fink, W. Zoller, *Makromol. Chem.* **1981**, *182*, 3265–3278. K. Soga, H. Yanagihara, D. Lee, *Makromol. Chem.* **1989**, *190*, 995. K. H. Reichert, K. R. Meyer, *Makromol. Chem.* **1973**, *169*, 163–176.
[35] B. Rieger, C. Janiak, *Angew. Makromol. Chem.* **1994**, *215*, 35–46.
[36] A. R. Siedle, R. A. Newmark, J. N. Schroepfer, P. A. Lyon, *Organometallics* **1991**, *10*, 400–404. A. R. Siedle, R. A. Newmark, W. M. Lamanna, J. N. Schroepfer, *Polyhedron* **1990**, *9*, 301–308. W. Kaminsky, R. Steiger, *Polyhedron* **1988**, *7*, 2375–2381. F. S. Dyachkovskii, A. K. Shilova, A. E. Shilova, *J. Polym. Sci.: Part C* **1967**, *16*, 2333–2339. G. Natta, G. Mazzanti, *Tetrahedron* **1960**, *8*, 86–100. D. S. Breslow, N. R. Newburg, *J. Am. Chem. Soc.* **1959**, *81*, 81–86. G. Natta, P. Pino, G. Mazzanti, U. Giannini, *J. Am. Chem. Soc.* **1957**, *79*, 2975–2976.
[37] A. R. Barron, *J. Chem. Soc., Dalton Trans.* **1988**, 3047–3050.
[38] C. Janiak, K. C. H. Lange, P. Marquardt, R.-P. Krüger, manuscript in preparation.
[39] H.-H. Brintzinger, D. Fischer, R. Mühlhaupt, B. Rieger, R. Waymouth, *Angew. Chem. Int. Ed. Engl.* **1995**, *34*, 1143–1170.
[40] W. A. Herrmann, J. Rohrmann, E. Herdtweck, W. Spaleck, A. Winter, *Angew. Chem. Int. Ed. Engl.* **1989**, *28*, 1511–1512.
[41] For a review on pyrrolyl or azacyclopentadienyl metal complexes, see: C. Janiak, N. Kuhn, *Advances in Nitrogen Heterocycles*, Vol II (C. J. Moody, ed.), JAI Press, Greenwich, CT, USA, **1996**, Vol. 2, 179–210.
[42] Q. Wang, R. Quyoum, D. J. Gillis, M.-J. Tudoret, D. Jeremic, B. K. Hunter, M. C. Baird, *Organometallics* **1996**, *15*, 693–703.
[43] W. Kaminsky, M. Miri, H. Sinn, R. Woldt, *Macromol. Chem. Rapid Commun.* **1983**, *4*, 417–424. W. Kaminsky, K. Külper, S. Niedoba, *Macromol. Chem. Macromol. Symp.* **1986**, *3*, 377–387.
[44] J. C. W. Chien, B.-P. Wang, *J. Polym. Sci. A: Polym. Chem.* **1988**, *26*, 3089–3102. W. Kaminsky, *Macromol. Symp.* **1995**, *97*, 79–89.
[45] P. Courtot, R. Pichon, J. Y. Salaun, L. Toupet, *Can. J. Chem.* **1991**, *69*, 661–672.
[46] P. T. Wolzanski, J. E. Bercaw, *Organometallics* **1982**, *1*, 793–799.
[47] J. M. Manriquez, D. R. McAlister, E. Rosenberg, A. M. Shiller, K. L. Williamson, S. I. Chan, J. E. Bercaw, *J. Am. Chem. Soc.* **1978**, *100*, 3079–3083.
[48] P. Renaut, G. Tainturier, B. Gautheron, *J. Organomet. Chem.* **1978**, *148*, 35–42.
[49] M. F. Lappert, C. J. Pickett, P. I. Riley, P. I. W. Yarrow, *J. Chem. Soc., Dalton Trans.* **1981**, 805–813.
[50] R. Riemschneider, *Z. Naturforsch.* **1963**, *B18*, 641–645. C. G. Vernier, E. W. Casserly, *J. Am. Chem. Soc.* **1990**, *112*, 2808–2809.
[51] E. C. Lund, T. Livinghouse, *Organometallics* **1990**, *9*, 2426–2427.
[52] H. Sitzmann, P. Zhou, G. Wolmershäuser, *Chem. Ber.* **1994**, *127*, 3–9.
[53] I. F. Urazowski, V. I. Ponomaryev, I. E. Nifant'ev, D. A. Lemenovskii, *j. Organomet. Chem.* **1989**, *368*, 287–294.
[54] S. Lasserre, J. Derouault, *Nouv. J. Chim.* **1983**, *7*, 659–665.
[55] A. D. Bacon, M. C. Zerner, *Theor. Chim. Acta* **1979**, *53*, 21–54. M. C. Zerner, *Reviews in Computational Chemistry, Vol. II.* (K. B. Lipkowitz, D. B. Boyd, Eds.), VCH Weinheim, **1991**, p. 313–365.
[56] R. Hoffmann, *J. Chem. Phys.* **1963**, *39*, 1397–1412. R. Hoffmann, W. N. Lipscomb, *J. Chem. Phys.* **1962**, *36*, 2179–2189. R. Hoffmann, W. N. Lipscomb, *J. Chem. Phys.* **1962**, *37*, 2872–2883.
[57] J. H. Ammeter, H.-B. Bürgi, J. C. Thibeault, R. Hoffmann, *J. Am. Chem. Soc.* **1978**, *100*, 3686–3692.
[58] C. Mealli, D. M. Proserpio, *J. Chem. Ed.* **1990**, *67*, 399–402.
[59] K. Tatsumi, A. Nakamura, P. Hofmann, P. Stauffert, R. Hoffmann, *J. Am. Chem. Soc.* **1985**, *107*, 4440–4451.
[60] R. H. Summerville, R. Hoffmann, *J. Am. Chem. Soc.* **1976**, *98*, 7240–7254.
[61] C. C. J. Roothaan, *Rev. Mod. Phys.* **1951**, *23*, 69.
[62] M. F. Guest, J. Kendrick, *GAMESS Users Manual*, SERC Daresbury Laboratory, CCP1/86/1, **1986**. M. Dupois, D. Spangler, J. J. Wendoloski, NRCC Software Catalog, Vol. 1, Program No. QG01 (GAMESS), **1980**. M. F. Guest, R. J. Harrison, J. H. van Lenthe, L. C. H. van Corler, *Theor. Chim. Acta* **1980**, *71*, 117.
[63] W. J. Hehre, R. F. Stewart, J. A. Pople, *J. Chem. Phys.* **1969**, *51*, 2657. W. J. Hehre, R. Ditchfield, R. F. Stewart, J. A. Pople, *J. Chem. Phys.* **1970**, *52*, 2769. W. J. Pietro, W. J. Hehre, *J. Comput. Chem.* **1983**, *4*, 241. J. B. Collins, P. v. R. Schleyer, J. S. Binkley, J. A. Pople, *J. Chem. Phys.* **1976**, *64*, 5142. H. Tatewaki, S. Huzinaga, *J. Chem. Phys.* **1980**, *72*, 399.
[64] J. S. Binkley, J. A. Pople, W. J. Hehre, *J. Am. Chem. Soc.* **1980**,

102, 939. M. S. Gordon, J. S. Binkley, J. A. Pople, W. J. Pietro, W. J. Hehre, *J. Am. Chem. Soc.* **1980**, *104*, 2797. M. J. Frisch, J. A. Pople, J. S. Binkley, *J. Chem. Phys.* **1984**, *80*, 3265. K. D. Dobbs, W. J. Hehre, *J. Comput. Chem.* **1986**, *7*, 359 and **1987**, *8*, 861, 880.

[65] T. H. Dunning Jr., P. J. Hay in *Modern Theoretical Chemistry*, Vol. 3, H. F. Schaefer ed., Plenum, New York, **1977**, p. 1.

[66] G. M. Sheldrick, *SHELXL-93*, Program for Crystal Structure Refinement, Göttingen, **1993**; *SHELXS-86*, Program for Crystal Structure Solution, Göttingen, **1986**.

[67] Further details of the crystal structure investigations may be obtained from the Fachinformationszentrum Karlsruhe, D-76344 Eggenstein-Leopoldshafen (Germany), on quoting the depository number CSD-405685.

[96130]